Bricheno, Lucy M.; Soret, Albert; Wolf, Judith; Jorba, Oriol; Baldasano, Jose Maria. 2013 Effect of High-Resolution Meteorological Forcing on Nearshore Wave and Current Model Performance. *Journal of Atmospheric and Oceanic Technology*, 30 (6). 1021-1037. 10.1175/JTECH-D-12-00087.1

Effect of High-Resolution Meteorological Forcing on Nearshore Wave and Current Model Performance

LUCY M. BRICHENO

National Oceanography Centre, Liverpool, United Kingdom

ALBERT SORET

Barcelona Supercomputing Centre, Barcelona, Spain

JUDITH WOLF

National Oceanography Centre, Liverpool, United Kingdom

ORIOL JORBA AND JOSE MARIA BALDASANO

Barcelona Supercomputing Centre, Barcelona, Spain

(Manuscript received 3 May 2012, in final form 28 February 2013)

ABSTRACT

Accurate representation of wind forcing and mean sea level pressure is important for modeling waves and surges. This is especially important for complex coastal zone areas. The Weather Research and Forecasting (WRF) model has been run at 12-, 4-, and 1.33-km resolution for a storm event over the Irish Sea. The outputs were used to force the coupled hydrodynamic and the Proudman Oceanographic Laboratory Coastal Ocean Modeling System (POLCOMS)–Wave Model (WAM) and the effect on storm surge and waves has been assessed. An improvement was observed in the WRF model pressure and wind speed when moving from 12- to 4-km resolution with errors in wind speed decreasing more than 10% on average. When moving from 4 to 1.33 km no further significant improvement was observed. The atmospheric model results at 12 and 4 km were then applied to the ocean model. Wave direction was seen to improve with increased ocean model resolution, and higher-resolution forcing was found to generally increase the wave height over the Irish Sea by up to 40 cm in places. Improved clustering of wave direction was observed when 4-km meteorological forcing was used. Large differences were seen in the coastal zone because of the improved representation of the coastline and, in turn, the atmospheric boundary layer. The combination of high-resolution atmospheric forcing and a coupled wave–surge model gave the best result.

1. Introduction

Close to the coast the interaction between wind, waves, and tides becomes most complex but also most critical. Storms are particularly important at the coast as these events can lead to high waves, storm surges, inundation, and erosion in populated areas. The motivation for this paper is to explore ways of improving coastal surge and wave forecasting by improving the atmospheric forcing. Here, we specifically examine the issue of atmospheric model resolution. Storm surges are generated by atmospheric pressure gradients and surface wind stress. In the deep ocean the main forcing is the inverse barometer effect since the large water depth and lack of coastal boundaries make wind stress ineffective at surge setup. Surges at the coast are produced by Ekman dynamics, behaving as forced Kelvin waves (Gill 1982). The most important mechanism for coastal surge generation is wind stress acting over shallow water. The size of the surge is proportional to the wind stress divided by the water depth and thus the same wind stress will lead to a larger surge in the shallowest regions such as the southern North Sea and eastern Irish Sea. Here, we are

Corresponding author address: Lucy M. Bricheno, National Oceanography Centre, Joseph Proudman Building, 6 Brownlow Street, Liverpool L3 5DA, United Kingdom.
E-mail: luic@noc.ac.uk

DOI: 10.1175/JTECH-D-12-00087.1

interested in the effect of midlatitude storms that can be assessed using coastal impact models of surges and waves when forced by extreme winds.

Problems in modeling storms can be related to the smoothness of modeled wind fields because of the limitations of spatial resolution not capturing secondary depressions, fronts, and the sting jet phenomenon (Browning 2004). Improved atmospheric model resolution has been found to improve the representation of storms, producing sharper mesoscale features as well as better representing convective events (Mass et al. 2002). Wolf and Flather (2005) discuss the problems of reconstructing the winds for the 1953 storm, which led to the largest coastal flooding disaster in the North Sea, because of surges and waves, in recent years. Even with the best available wind reconstruction, the first surge peak on the eastern coast of England late on 31 January was not reproduced, most probably because of deficiencies in the wind data (Wolf and Flather 2005). Work by Heaps (1983) referring back to Lennon (1963) showed that surges on the western coast of the United Kingdom are related to the track and speed of secondary depressions. The storm characteristics for west coast surges [typical wind speeds ≈ 40 kt (1 kt = 0.51 m s^{-1}) and surge elevations of 2.5 m] were revisited by Brown et al. (2010b). Ardhuin et al. (2007) and Bertotti et al. (2012) have found substantial differences between the results of different operational models of wind and waves for an extreme storm in the western Mediterranean Sea concerning the peak values of wind speed and significant wave height, the general distribution of the fields, and the locations of the maxima. Miller et al. (2010) describe the improvements in integrated forecast system (IFS) skills during the last resolution increase performed with the global model at the European Centre for Medium-Range Weather Forecasts (ECMWF).

Various studies have identified the need for good spatial resolution of the storm to get the maximum wind correct (e.g., Cavaleri 2009) in order to get accurate wave forecasts. Apart from the correct value of the mean wind speed, it is also important to get the correct gustiness, which is the turbulence in the wind because of the friction in the surface boundary layer. Typical monthly root-mean-square (RMS) errors in the U.K. operational storm surge model are of the order 0.1 m, but maximum instantaneous errors can be as large as 0.5 m (Wortley et al. 2007). Whether this reflects a deficiency in the physics of the surge model or a natural limit of predictability because of the resolution (0.11°) of the atmospheric model is unclear. The recent works of Maskell (2012) and O'Neill et al. (2012) highlight the need for high-resolution surface forcing for accurate Irish Sea modeling.

Increased resolution requires the use of topography maps of $\leq$1-km resolution and also resolves extra physical processes that are parameterized in coarser models. But what effect does the use of higher-resolution topography have on the smaller-scale meteorological features and thus the ocean? The Weather Research and Forecasting (WRF) model has been used to simulate coastal meteorology in several regions (Caldwell et al. 2009; Jorba et al. 2008; Floors et al. 2011) with Jorba et al. (2008) highlighting problems with the model when simulating complex terrain and coastal areas, which will also be discussed in the present work. One of the issues for numerical weather prediction is the downscaling of global model predictions to regional and local scales via model nesting. This approach must simultaneously predict both global and synoptic weather patterns (which have scales of the order of 1000 km) and also downscale these to yet finer scales. A two-way coupling between the model nest levels also permits feedback from the small to the large scales. However, a discussion of the impact of using WRF for precipitation modeling within a climate model system is given by Bukovsky and Karoly (2009), which suggests that the two-way feedback may not be beneficial.

The body of evidence supporting coupled ocean–atmosphere modeling has been steadily growing (Hodur 1997; Seo et al. 2007; Warner et al. 2008, 2010; Bertotti et al. 2012). Each component of a coupled atmosphere, hydrodynamic, and wave modeling system needs to be well understood and validated; otherwise, errors can propagate from one system to another. The ocean model depends on outputs from the atmospheric model as a driver and receives wind speed and direction, sea level pressure, temperature, humidity, cloud cover, and evaporation minus precipitation rate from the meteorological model. There is also scope for including feedbacks from ocean to atmosphere; the most important fields to consider are sea surface temperature, relative wind speed, and sea state. Relative wind speed has already been included in the Proudman Oceanographic Laboratory Coastal Ocean Modeling System (POLCOMS)–Wave Model (WAM; Osuna and Wolf 2005), and wave-based surface roughness was included in POLCOMS by Brown and Wolf (2009). The impact of sea surface temperature on the atmosphere has been investigated by many authors (e.g., Seo et al. 2007) and found to have important effects on surface wind and heat fluxes.

The objective of this work is to study the impact of using high-resolution modeling on 1) coastal meteorology and 2) the response of the coastal ocean to high-resolution meteorology, as well as increased ocean model resolution. As a test bed, the coastal area of the eastern Irish Sea including Liverpool Bay is targeted. The Irish Sea is subject to severe winter storms, with the Isle of Man experiencing around 10–15 days of gale per year (Met Office 2013). Winds have an annual average surface

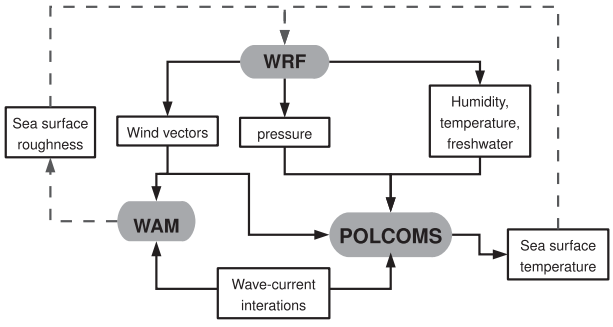

FIG. 1. Model schematic showing components in gray boxes and variables passed in black arrows. Some potential pathways for future work are shown by dashed lines.

speed of $5\,\mathrm{m\,s^{-1}}$, but in severe storms (e.g., January 2012) the maximum gust speed at Liverpool can exceed $30\,\mathrm{m\,s^{-1}}$. These winds are associated with the right rear quadrant of midlatitude depressions, which track across the United Kingdom from the North Atlantic (Brown et al. 2010a,b). The coastal zone is dominated by turbulent flows, often thermally driven by sharp gradients at the coastline. Liverpool Bay is exposed to the prevailing southwesterly winds and depressions moving across the United Kingdom from west to east. The coastal zone is well monitored, as it is also known to be at risk from coastal flooding (Wolf 2008). This paper begins by detailing the components of the modeling system used and describes the model configurations in section 2. In section 3, the study period is outlined. In section 4, results from the meteorological model are presented and assessed at several observational stations. The meteorological model outputs were used to drive the coupled ocean model applied to the study area of Liverpool Bay. Section 5 assesses the performance of the ocean model, evaluating wave conditions and coastal surge elevations. The main findings are discussed in section 6 with suggestions for future work in section 7. Finally, the work is summarized in section 8.

2. Methods

Three well-established models have been used: an ocean basin–scale spectral wave model, which has been coupled with a 3D tide and surge model, POLCOMS (Osuna and Wolf 2005). For the atmospheric modeling, a version of the Advanced Research Weather Research and Forecasting model (ARW-WRF v3.2; Michalakes et al. 2004; Skamarock et al. 2008), hereafter referred to as WRF (detailed in section 2a), is used. The outputs from the meteorological model were used to drive both ocean models (detailed in section 2b) at a range of spatial resolutions. The model coupling presented in a flowchart in Fig. 1 shows the variables shared between models. Currently, the coupling is performed ''offline'' with the atmospheric model being run first, then passing fields to the ocean models. A long-term aim for this system would be to run the models concurrently, passing variables between the ocean and atmosphere models more frequently and creating a tighter coupling. To analyze the model performance the coefficient of correlation (R^2), RMS error, and percentage model bias (Pbias), defined as

$$\mathrm{Pbias} = 100\frac{\sum_{n=1}^{N}(M_n - D_n)}{\sum_{n=1}^{N}(D_n)}, \tag{1}$$

will be calculated. The model prediction is represented by M, D represents the measured data, and N is the total number of data points used to calculate the cost function. The RMS presents an absolute error for the model data, R^2 is an indicator of how much of the variance is explained by the correlation, and Pbias provides a measure of whether the model is systematically over or under predicting the measured data. As a measure of goodness of fit, a cost function (CF) is also defined, as

$$\mathrm{CF} = \sqrt{\frac{1}{N\sigma_D^2}\sum_{n=1}^{N}(M_n - D_n)^2}, \tag{2}$$

where σ_D represents the standard deviation of the data. For all statistical calculations, hourly data are extracted from the model throughout the 9-day study period, giving a pool of 216 points. The observational data ranges in temporal resolution between 10 min (at the wind farm and coastal sites) to hourly at the inland sites.

a. Meteorological modeling

The meteorological model (WRF; Skamarock et al. 2008) was run for the 9-day study period, reinitializing the model from global data daily to avoid excessive drift. As well as being run at different model resolutions, WRF was run in a one- and two-way nested configuration. Model nesting helps with the evaluation of small-scale processes within the larger-scale flow. The physical parameterizations used are the Yonsei University planetary boundary layer model (Hong et al. 2006), WRF single-moment 3-class microphysics scheme (Dudhia 1989; Hong et al. 2004), Kain–Fritsch cumulus scheme (Kain 2004), the Noah land surface model (Ek et al. 2003), Rapid Radiative Transfer Model for longwave radiation (Mlawer et al. 1997), and the Dudhia scheme for shortwave radiation (Dudhia 1989).

Boundary conditions are supplied at 6-hourly intervals from the global analyses model [National Centers for

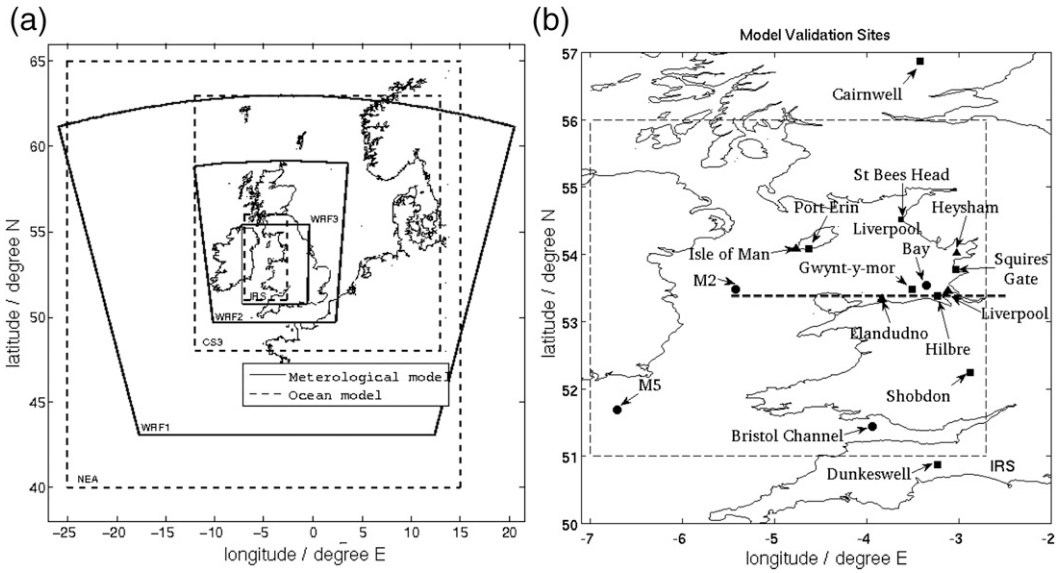

FIG. 2. Extent of the (a) model domain nests used and (b) validation sites used. In (b) the location of several validation points are marked; buoys are circles, tide gauges are triangles, and meteorological stations are marked with squares. The line taken by the vertical sections in Fig. 5 is plotted as a thick dashed line in (b).

Environmental Prediction Final (NCEP FNL)] at 1° × 1° spatial resolution. The model is run for 12 h to spin up the outer domain and then for a further 24 h to produce output data. The atmospheric planetary boundary layer was represented by 12 sigma levels below the 850-hPa level, with the lowest level set at 38 m AGL. Authors consider that such vertical configuration can correctly reproduce atmospheric dynamics in a complex coastal area. Marrero et al. (2009) found a lack of sensitivity by increasing the vertical levels from 31 to 61 in their case study in similarly stormy conditions and very complex topography (Tenerife). The meteorological model is configured with 32 vertical sigma levels, and the top of the atmosphere is set as 50 hPa. The atmospheric planetary boundary layer was represented by 12 sigma levels below the 850-hPa level, with the lowest level set at 38 m AGL. It should also be noted that Marrero et al. (2009) found a lack of sensitivity to the number of vertical levels in their case study, a similarly stormy environment.

The model resolution increases from 12 km in the outer domain to 4 km in the intermediate and 1.33 km in the finest domain. The resolution of the underlying terrain is also increased from 0.166° in the 12-km model (WRF1) to 2 min in the 4-km model (WRF2). The highest-resolution meteorological model (WRF3) uses a terrain resolution of 30 s.

b. Ocean modeling

For the ocean component of this study the POLCOMS (Holt and James 2001) is used, coupled with the third-generation spectral wave model (WAM; Komen et al. 1994), modified for shallow water (Monbaliu et al. 2000). A 1.8-km Irish Sea (IRS) domain is used, as previously described in Brown et al. (2010a). The extent of this and all outer model domains are plotted in Fig. 2a. For all model domains, a minimum water depth of 10 m was imposed to avoid the implementation of wetting and drying at the coast. The outer model was used to generate tide and surge boundary conditions for the Irish Sea model.

To initialize the ocean models, a few days to a week is required for spinup. The previous month (November 2006) was available from another study and the ocean model was initialized using this data. As the meteorological model was not run for this spinup period, another atmospheric dataset was needed to force the ocean over this spinup period. The Met Office northwest European continental shelf (mesoscale) model with a resolution of ≈0.11° was used to drive the November simulation. Once spun up, the ocean models were then forced with the 9 days of output from the WRF model. The ocean modeling component was forced at the open boundary with an northeast Atlantic (NEA) wave model and a 15-constituent tidal model.

The NEA model is forced with 6-hourly 40-yr ECMWF Re-Analysis (ERA-40) winds and pressure data at a 1° resolution, provided by the European Centre for Medium-Range Weather Forecasts. This is usually necessary to provide incoming swell waves, although in our study region Liverpool Bay is not significantly affected by swell (Wolf et al. 2011). To force the local ocean model, a mean sea level pressure and 10-m wind are

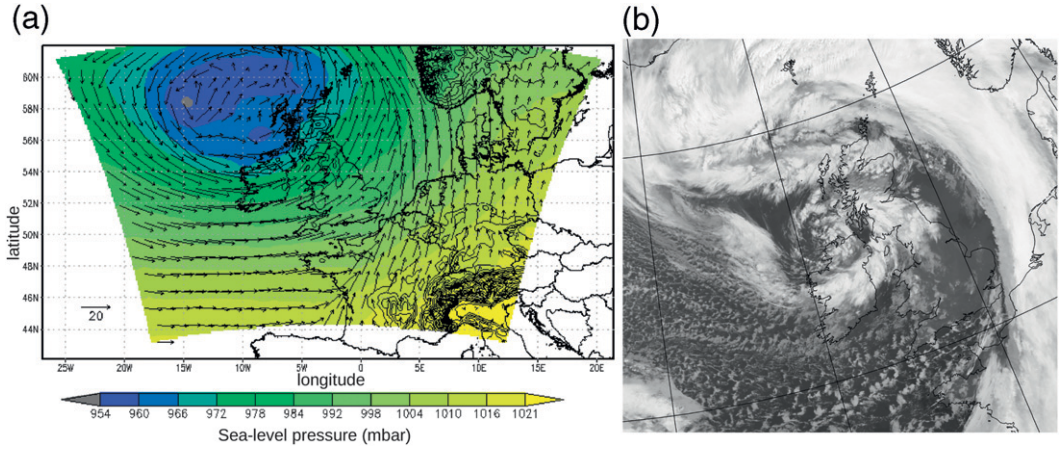

FIG. 3. (a) Sea level pressure (colors) and 10-m winds (vectors) from the 12-km WRF model and (b) an infrared AVHRR satellite observation for a snapshot during the study period 1200 UTC 3 Dec 2006, courtesy of the Natural Environment Research Council (NERC) Satellite Receiving Station, Dundee University, Scotland.

derived from the meteorological model output. Both one- and two-way nested meteorological model configurations at 12- and 4-km resolution were used to force the ocean models. The effect of variable ocean model resolution was investigated as well as atmospheric model resolution. The performance of the wave and surge models is assessed in section 5 at both 12- and 1.8-km resolution.

3. Study period

On the northwest European continental shelf the largest wind speeds are associated with midlatitude depressions (otherwise known as extratropical cyclones) typically tracking across the United Kingdom from southwest to northeast. Surges are largest where these storms impact large areas of shallow continental shelves and determination of coastal wind stress is critical (Wolf 2009). As a case study, a 9-day period at the beginning of December 2006 was chosen (from 1 to 9 December). At this time a storm event crossed the northern British Isles. From the synoptic point of view, this period is dominated by three low pressure systems (LPSs) affecting the area of study. The three LPSs arrived at the Liverpool Bay buoy at 1200 UTC 3 December 2006, 0000 UTC 5 December 2006, and 2300 UTC 7 December 2006, respectively. The synoptic situation is presented in Fig. 3, which shows modeled sea level pressure and an Advanced Very High Resolution Radiometer (AVHRR) image taken at 1200 UTC 3 December 2006. The trajectories of the first two storms are from west to east, producing strong southwesterly winds (20–15 m s^{-1}). The third system has weaker winds (10 m s^{-1}), mainly northwesterly. The period is characterized by synoptic southwesterly winds through the lower troposphere.

4. Meteorological model results

In this section, the wind field results are evaluated against surface observations. Model results are compared against observations at five offshore, four coastal, and three land-based stations (Fig. 2b). Three representative stations are selected to analyze the evolution of the winds for the period of study:

- Gwynt-y-mor: This station is located at the site of a proposed wind farm 18 km off the northern Wales coast. The offshore location represents a flat surface with homogeneous surface conditions.
- Hilbre Island: This is a coastal station located on a small island (80 × 500 m) of elevation 6 m located around 2 km offshore in the mouth of the river Dee. This station is expected to be significantly influenced by the changes in surface properties from land to sea.
- Dunkeswell Aerodrome (Devon): This station is located inland around 20 km from the coast with an elevation of 252 m. Dunkeswell is situated in a flat land area surrounded by homogeneous smooth topography.

Figure 4 shows wind speed time series of the two-way nested configuration at the three selected sites compared with observations. The dots represent observations and the different lines are the model results for the WRF1, WRF2, and WRF3 domains. The offshore location Gwynt-y-mor (Fig. 4a) results show a good agreement with observations (with the model explaining between 0.57 and 0.67 of the wind speed variability). Some overestimation is observed during low wind

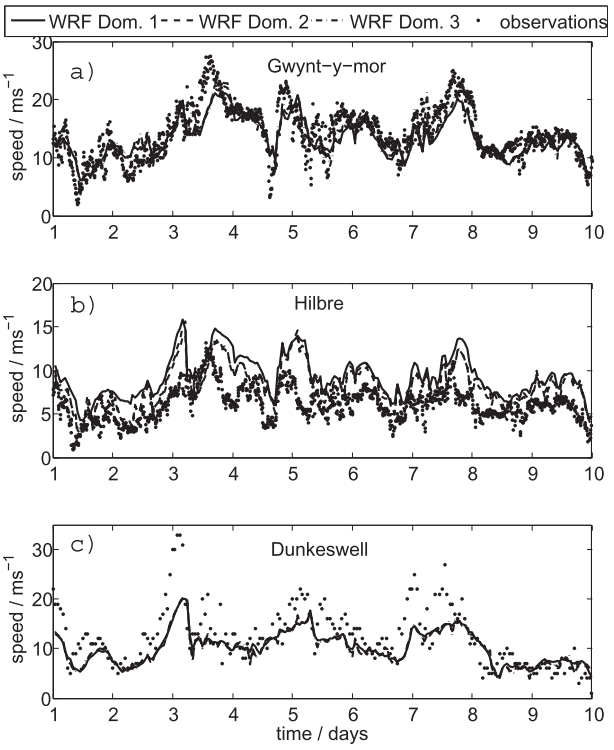

FIG. 4. Time series of modeled wind speed from two-way nested WRF simulations, at (a) Gwynt-y-mor wind farm, (b) Hilbre, and (c) Dunkeswell. The time series cover the full study period 1–10 Dec 2006. Note different scales for wind speed are used to best display the variability at each site.

episodes, but the strong wind conditions are well captured with the maximum bias remaining below $2\,\mathrm{m\,s^{-1}}$ throughout most of the simulation period. There is no consistent difference between the model outputs at different resolutions. At the coast, the modeled wind speed at Hilbre Island captures more than half of the variability, but the model slightly overestimates the observations (Fig. 4b). The increase of resolution helps to reduce the overestimate of these peaks. Inland, at Dunkeswell the homogeneous and relatively smooth topography explains the fact that there are no significant differences between the different model resolutions (Fig. 4c).

The selected stations are located within all WRF domains (plotted in Fig. 2) of the meteorological simulation, and thus, meteorological results at different horizontal resolutions can be compared. The model explains between 0.48 and 0.55 of the wind speed variability at all sites. When results from two-way versus one-way coupling were compared, the models behaved very similarly, with a maximum difference in wind speed of $0.05\,\mathrm{m\,s^{-1}}$; so for the remaining comparison only the two-way nested results will be described in detail. When moving from 4- to 1.33-km resolution, wind speed correlations were not seen to improve significantly. The NCEP FNL (run at 1°) is probably too coarse a resolution to downscale as far as 1.33 km, and therefore results from the two coarser (12 and 4 km) domains will be the focus of the paper.

Tables 1, 2, 3, and 4 present a quantitative evaluation of the wind speeds and directions compared with data for a total of 12 sites, including the three detailed in Fig. 4. Biases for wind speed are presented in Table 5. The inland points give consistent results for different model resolutions, and this is reflected in the R^2 values, with the RMS errors neither improving nor deteriorating with a higher resolution. The wind speeds over land are consistently underpredicted (−26.1% on average) with negative Pbias seen at all model sites and all resolutions. The coastal sites at Hilbre Island and the Isle of Man are less well correlated but are slightly improved on moving from 12- to 4-km resolution. The absolute errors are actually smaller than those seen inland (mean coastal RMS error 2.8 versus land RMS error 4.1), but the model biases are more variable with both under- and overprediction of wind speeds seen, which is thought to be caused by poor resolution of the coastline. The worst correlations are found with the buoy stations. However, the Gwynt-y-mor site (which is also offshore) has a much better value of R^2 because it is recorded at a fixed mast. This is reflected in the model biases as well, where Gwynt-y-mor has more in common with the coastal stations. Modeled wind speeds at buoy sites are predicted to be up to 50% smaller than those observed in the data, while at Gwynt-y-mor the bias is reduced to 15%. The poor result offshore compared to buoy observations may be because of a discrepancy between the heights at which data are collected and the uncertainties associated with buoy data (Pickett et al. 2003). The Irish Marine Institute buoys (M2 and M5) record data at 4.5 m above the sea surface. However, these observations are then being compared directly with winds modeled at 10 m above the sea surface.

When the spatial resolution is increased in coastal areas, two obvious improvements are observed. First, it helps to better characterize the coastline. The sharp transition in bottom roughness when moving from land to sea cannot be captured at low spatial resolution. Second, lower resolution implies a smoothing of the orography and an underestimation of the roughness of the surface. Both aspects are exemplified in Figs. 5d, 5e, and 5f, where the increase of the resolution helps to realistically define orography. Figures 5a, 5b, and 5c show vertical cross sections of the wind speed at Hilbre Island for the first storm event (0800 UTC 3 December) at the three spatial resolutions. Over the Irish Sea, west of 5.0°W (not shown), no significant differences are

TABLE 1. The R^2 values for wind speed ($m\,s^{-1}$) at 12 observation sites at three different resolutions, comparing one- and two-way model coupling. The land sites are italicized, sea sites are in bold, and coastal points are unhighlighted.

Location			12 km	4 km	1.33 km	12 km	4 km	1.33 km
Resolution	Lat °N	Lon °E	Two-way			One-way		
Dunkeswell	50.87	−3.23	*0.64*	*0.68*	—	*0.69*	*0.64*	—
Cairnwell	56.88	−3.42	*0.47*	*0.54*	—	*0.52*	*0.55*	—
Shobdon	52.25	−2.88	*0.57*	*0.56*	*0.51*	*0.61*	*0.64*	*0.64*
Hilbre	53.38	−3.23	0.47	0.54	0.53	0.55	0.56	0.56
Squires Gate	53.77	−3.03	0.66	0.67	0.64	0.66	0.73	0.64
St Bees Head	54.52	−3.63	0.57	0.66	0.66	0.70	0.69	0.66
Isle of Man	54.08	−4.63	0.48	0.55	0.54	0.49	0.53	0.55
Gwynt-y-mor	53.48	−3.51	**0.57**	**0.67**	**0.65**	**0.59**	**0.67**	**0.63**
M2	53.48	−5.43	**0.32**	**0.45**	**0.31**	**0.47**	**0.45**	**0.32**
M3	51.26	−10.55	**0.37**	—	—	**0.41**	—	—
M4	55.00	−10.00	**0.41**	—	—	**0.56**	—	—
M5	53.07	−5.88	**0.31**	**0.32**	**0.32**	**0.39**	**0.42**	**0.37**
Average			0.48	0.55	0.52	0.50	0.52	0.55

observed between model resolutions. From west to east, over the Irish Sea (5.5°–4.5°W), no significant differences are observed between model resolutions. Over the coastal area in northern Wales (4.5°–3.0°W) more differences are observed. As summarized earlier, this period is characterized by southwesterly winds and this area is leeward of the Welsh mountains. The increase in resolution allows better reproduction of the influence of the orography and higher wind speeds are observed. For Liverpool Bay (3.0°W), atmosphere–land interactions produce a reduction of the wind velocity that is well observed with the increase of the resolution. Over land (3.0°–2.5°W), despite this being a very flat area, orographic influences are observed when increasing the spatial resolution, with the development of wake areas and gravity waves (not shown). Such vertical structures strongly contribute to the high winds developed within the area.

The mean absolute error in the wind speeds considering all 12 sites is $3.60\,m\,s^{-1}$ (see Table 3). This is a complex coastal area and so model results are typically less accurate than those seen over open water. This value is in good agreement with previous modeling studies (e.g., Floors et al. 2011).

Modeled wind direction was also considered, with values for R^2 and RMS error presented in Tables 2 and 4, respectively. All model resolutions at the three study sites found too wide a spread of wind directions when compared with observations. This spread was reduced somewhat when moving to a higher resolution. In the observed winds, southeasterly winds were seen to be ''funneled'' by the Dee estuary. However, this signal was not observed at any resolution in the model simulations of this study. Wind directions are better correlated than wind speeds at all sites, with an average of 0.73 for direction compared with 0.52 for speeds (across all model

TABLE 2. The R^2 values for wind direction at 12 observation sites at three different resolutions, comparing one- and two-way model coupling. The land sites are italicized, sea sites are in bold, and coastal points are unhighlighted.

Location			12 km	4 km	1.33 km	12 km	4 km	1.33 km
Resolution	Lat °N	Lon °E	Two-way			One-way		
Dunkeswell	50.87	−3.23	*0.47*	*0.74*	—	*0.68*	*0.67*	—
Cairnwell	56.88	−3.42	*0.54*	*0.76*	—	*0.76*	*0.75*	—
Shobdon	52.25	−2.88	*0.54*	*0.60*	—	*0.56*	*0.56*	—
Hilbre	53.38	−3.23	0.65	0.86	0.85	0.86	0.87	0.84
Squires Gate	53.77	−3.03	0.76	0.84	0.83	0.85	0.87	0.83
St Bees Head	54.52	−3.63	0.71	0.83	0.83	0.86	0.86	0.84
Isle of Man	54.08	−4.63	0.39	0.65	0.65	0.62	0.62	0.67
Gwynt-y-mor	53.48	−3.51	**0.65**	**0.90**	**0.90**	**0.88**	**0.88**	**0.89**
M2	53.48	−5.43	**0.88**	**0.84**	**0.68**	**0.75**	**0.88**	**0.70**
M3	51.26	−10.55	**0.66**	—	—	**0.45**	—	—
M4	55.00	−10.00	**0.85**	—	—	**0.82**	—	—
M5	53.07	−5.88	**0.76**	**0.55**	**0.51**	**0.61**	**0.64**	**0.57**
Average			0.64	0.76	0.75	0.73	0.76	0.76

TABLE 3. RMS error values for wind speed ($m\,s^{-1}$) at 12 observation sites at three different resolutions, comparing one- and two-way model coupling. The land sites are italicized, sea sites are in bold, and coastal points are unhighlighted.

Location			12 km	4 km	1.33 km	12 km	4 km	1.33 km
Resolution	Lat °N	Lon °E	Two-way			One-way		
Dunkeswell	50.87	−3.23	*3.50*	*3.26*	—	*3.24*	*3.47*	—
Cairnwell	56.88	−3.42	*4.24*	*3.92*	—	*4.03*	*3.91*	—
Shobdon	52.25	−2.88	*4.38*	*4.44*	*4.66*	*3.99*	*4.19*	*3.99*
Hilbre	53.38	−3.23	1.40	1.31	1.31	1.65	1.61	1.75
Squires Gate	53.77	−3.03	4.59	4.53	4.75	4.64	4.13	4.72
St Bees Head	54.52	−3.63	2.46	2.18	2.17	3.97	4.07	4.28
Isle of Man	54.08	−4.63	2.98	2.75	2.79	2.94	2.82	2.76
Gwynt-y-mor	53.48	−3.51	**2.77**	**2.44**	**2.50**	**2.58**	**2.42**	**2.79**
M2	53.48	−5.43	**3.41**	**3.15**	**3.17**	**3.15**	**3.14**	**3.15**
M3	51.26	−10.55	**5.30**	—	—	**5.11**	—	—
M4	55.00	−10.00	**4.84**	—	—	**6.29**	—	—
M5	53.07	−5.88	**6.25**	**6.26**	**6.26**	**5.17**	**4.91**	**5.17**
Average			3.84	3.42	3.45	3.90	3.47	3.58

configurations). The reason that wind direction is better correlated than speed is because during a storm the synoptic pattern is dominating the flow and large-scale features are driving the wind direction. The opposite is true during the summer, when wind speeds are generated by more localized pressure gradients. The best agreement was found offshore at Gwynt-y-mor, where the model is able to explain 90% of the variability in wind direction. The RMS error in wind direction averaged around 30°, with the smallest errors found at the offshore sites (at Gwynt-y-mor the error was as small as 15°). Increased model resolution reduced the error by up to 8°, with the best improvements seen at the coastal sites.

The Pbias [Eq. (1)] was also calculated for wind direction at all sites. M2 and M5 see a positive bias of 15% and 17%, respectively. The best agreement is seen offshore at Gwynt-y-mor with a bias of −6%; this is also the site where the wind speeds were in best agreement. Inland at Dunkeswell, a directional bias of −13% is seen. The largest error is seen, as for the wind speeds, at Hilbre Island. Here a bias of +25% is observed. A systematic bias in the wind speed is observed inland, but this shortcoming should not impact our use of WRF as an ocean surface boundary forcing.

To summarize the meteorological model results, WRF was found to best simulate wind speed and direction when running at a 4-km resolution, with large errors at coastal points becoming reduced at a higher resolution. The increase of resolution is required in coastal areas where the land–atmosphere–ocean interactions become crucial.

5. Ocean model results

a. Waves

The POLCOMS–WAM model has been validated for this area in previous studies to investigate surge

TABLE 4. RMS error values for wind direction (°) at 12 observation sites at three different resolutions, comparing one- and two-way model coupling. The land sites are italicized, sea sites are in bold, and coastal points are unhighlighted.

Location			12 km	4 km	1.33 km	12 km	4 km	1.33 km
Resolution	Lat °N	Lon °E	Two-way			One-way		
Dunkeswell	50.87	−3.23	*34.39*	*20.74*	—	*23.66*	*23.14*	—
Cairnwell	56.88	−3.42	*47.34*	*32.62*	—	*33.42*	*33.54*	—
Shobdon	52.25	−2.88	*39.16*	*23.85*	—	*27.40*	*26.78*	—
Hilbre	53.38	−3.23	34.95	23.27	23.01	24.69	23.27	24.48
Squires Gate	53.77	−3.03	39.79	31.54	31.87	31.96	31.35	31.88
St Bees Head	54.52	−3.63	28.19	19.55	20.00	19.30	18.32	19.87
Isle of Man	54.08	−4.63	35.65	22.97	23.12	24.04	23.80	22.11
Gwynt-y-mor	53.48	−3.51	**26.50**	**14.21**	**13.92**	**15.27**	**15.21**	**14.90**
M2	53.48	−5.43	**19.52**	**16.16**	**22.98**	**20.89**	**14.68**	**22.34**
M3	51.26	−10.55	**27.49**	—	—	**33.54**	—	—
M4	55.00	−10.00	**26.18**	**47.37**	—	**23.17**	**46.12**	—
M5	53.07	−5.88	**25.84**	**30.01**	**31.65**	**28.94**	**26.82**	**29.28**
Average			32.08	25.66	23.79	25.52	25.73	23.55

TABLE 5. Pbias for wind speed ($m\,s^{-1}$) at 12 observation sites at three different resolutions, comparing one- and two-way model coupling. The land sites are italicized, sea sites are in bold, and coastal points are unhighlighted.

Location			12 km	4 km	1.33 km	12 km	4 km	1.33 km
Resolution	Lat °N	Lon °E	Two-way			One-way		
Dunkeswell	50.87	−3.23	*−19.71*	*−20.62*	—	*−18.23*	*−21.45*	—
Cairnwell	56.88	−3.42	*−46.93*	*−46.34*	—	*−43.33*	*−44.94*	—
Shobdon	52.25	−2.88	*−18.36*	*−19.37*	*−20.00*	*−10.82*	*−13.87*	—
Hilbre	53.38	−3.23	61.37	28.71	30.92	65.04	34.74	45.58
Squires Gate	53.77	−3.03	−47.73	−46.75	−47.83	−45.04	−45.96	−54.71
St Bees Head	54.52	−3.63	10.76	7.34	13.29	15.80	9.37	22.10
Isle of Man	54.08	−4.63	14.59	17.00	17.29	22.64	22.23	22.09
Gwynt-y-mor	53.48	−3.51	**14.05**	**16.57**	**16.96**	**18.72**	**16.37**	**15.70**
M2	53.48	−5.43	**−52.03**	**−47.95**	**−47.77**	**−50.72**	**−50.90**	**−51.67**
M3	51.26	−10.55	**−46.36**	—	—	**−45.97**	—	—
M4	55.00	−10.00	**−39.61**	—	—	**−39.09**	—	—
M5	53.07	−5.88	**−41.13**	**−41.27**	**−41.26**	**−40.88**	**−41.55**	**−41.11**
Average			−17.59	−15.27	−4.64	−14.32	−13.60	−0.11

elevations and wave–current interaction (Brown et al. 2010a). The aforementioned study used meteorological forcing from the Met Office northwest European continental shelf (mesoscale) model with a resolution of 12 km, and their model configuration was used as a starting point for this work. Brown et al. (2010a) found a cost function CF [Eq. (2)] less than 0.6, with Pbias [Eq. (1)] generally less than 30% and often less than 10% for POLCOMS. For WAM, a CF less than 0.7 is found for significant wave height and Pbias is less than 38%. Less than 10% is thought to be excellent, and 20%–40% is good. Brown et al. (2010b) also assessed the wave model

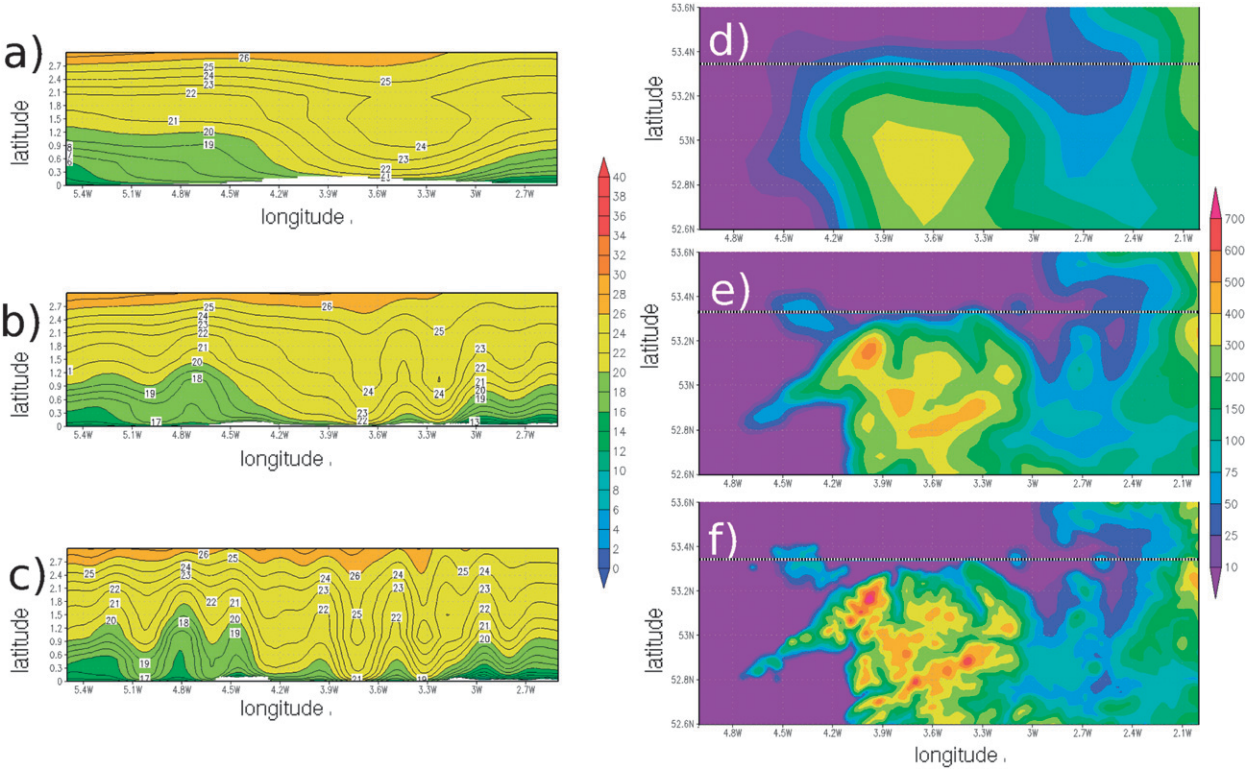

FIG. 5. Vertical sections of wind speed ($m\,s^{-1}$) taken at 53.3828°N, a section through Hilbre Island: (a) 12, (b) 4, and (c) 1.33 km. These sections were taken at 0800 UTC 3 Dec 2006. (d)–(f) The corresponding terrain height (m) at each model resolution, with the section marked with a dashed line.

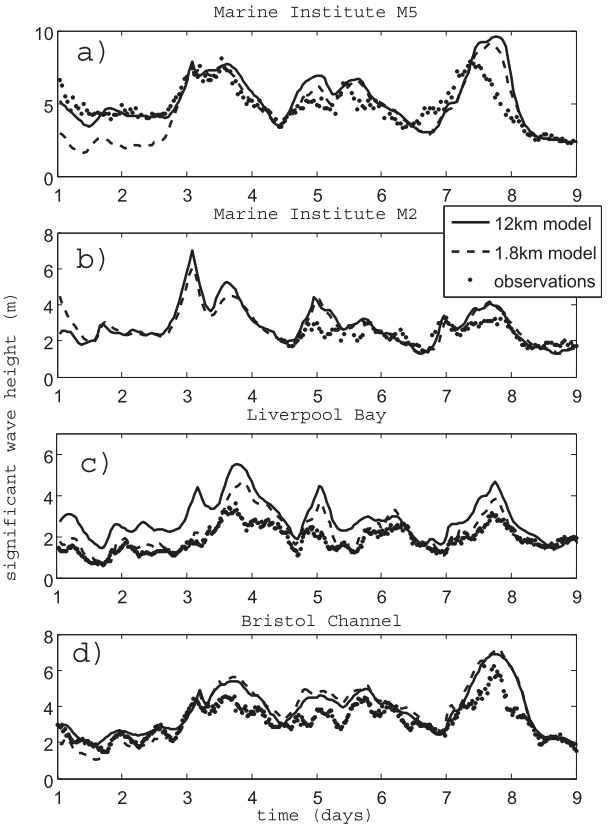

FIG. 6. Time series of significant wave height at four buoys in the Irish Sea comparing (a) M5, (b) M2, (c) Liverpool Bay, and (d) Bristol Channel. The 12-km (solid line) and 1.8-km model (dashed line) are compared with observations (points). In both cases, the 12-km resolution WRF output was used as atmospheric forcing, while the ocean model configuration remains constant.

hindcast performance at the Liverpool Bay buoy in 2006, finding a correlation of 0.93 with an RMS error of 0.38 m. The ocean wave and surge models were run in the same configuration several times but forced with different meteorological model outputs. Initially, the 12-km WRF model was used to force both ocean model resolutions, but the 4-km resolution WRF outputs were also tested to drive the 1.8-km ocean model. Outputs from both one- and two-way WRF configurations were also tested as forcings for the ocean models.

To assess the performance of the ocean models, observations from buoys and tide gauges have been used; a summary map of their locations is shown in Fig. 2b. Two nearshore WaveNet buoys in shallow water, Liverpool Bay (22 m) and Bristol Channel (28 m), are compared in Fig. 6, with two Irish Marine Institute buoys in deeper water, M2 (81 m) and M5 (74 m). Time series at the four sites are plotted, and some statistical analysis is summarized in Table 6. The wave conditions are well captured at all sites at both model resolutions

TABLE 6. The R^2 values, Pbias, and cost functions for significant wave height at four study sites at two different ocean model resolutions.

Resolution		12 km (CS3)			1.8 km (IRS)		
Location	Water depth	R^2	Pbias	CF	R^2	Pbias	CF
M2	81 m	0.5224	8.91	0.81	0.8209	11.13	0.86
M5	74 m	0.6325	9.43	1.23	0.5344	4.33	1.33
Liverpool Bay	22 m	0.4004	54.33	1.53	0.8091	18.96	0.71
Bristol Channel	28 m	0.8615	17.07	0.80	0.8392	16.11	0.96

with the models explaining 0.68 of the variability on average.

The wave height (Hs) is consistently overpredicted, particularly at Liverpool Bay in the 12-km continental shelf (CS3) ocean model where the average error is 87 cm, reducing to 41 cm in the finer model. In the Bristol Channel Hs is overpredicted by 93 cm in the coarse model, reducing to 51 cm in the IRS 1.8-km ocean model. This overprediction is related to the forcing, as the nearby wind speeds are also overpredicted (the Liverpool Bay buoy is very close to Hilbre Island). Offshore, the biases are reduced, with M5 overpredicted by 69 cm in the 12-km CS3 and by 43 cm in the finer IRS model. M2 is overpredicted by 53 cm at 12-km resolution and 27 cm in the 1.8-km model. The largest overprediction, and divergence between models, is seen in Liverpool Bay. Wolf et al. (2011), who use the same model configuration described here, also find the 1.8-km Irish Sea model underestimates the wave height in Liverpool Bay. They attribute this effect to an underestimate in model wind speed used as a forcing, which agrees with the findings of this study.

Next, the effect of running the same ocean model with variable-resolution atmospheric forcing is considered (Fig. 7). There is very little pointwise difference seen in simulated wave height (e.g., at the Liverpool Bay buoy the wave heights have a correlation of 0.97). When contrasting one-way and two-way nesting (Fig. 7b), little change is seen in the pointwise significant wave height (with a correlation of 93% Liverpool Bay); again the data from Liverpool Bay are shown. Figure 8 shows results from the high-resolution (1.8 km) wave model compared with those from the 12-km model. In all cases the modeled approach direction of the waves is found to be too much north of west. On increasing the model resolution, the spread of wave directions is focused to a narrower band, bringing the models closer to observations. At the Liverpool Bay site the spurious southwesterly waves were also reduced at a higher resolution. A bias was observed in the model wind roses (not shown) being rotated anticlockwise (i.e., too much from the north

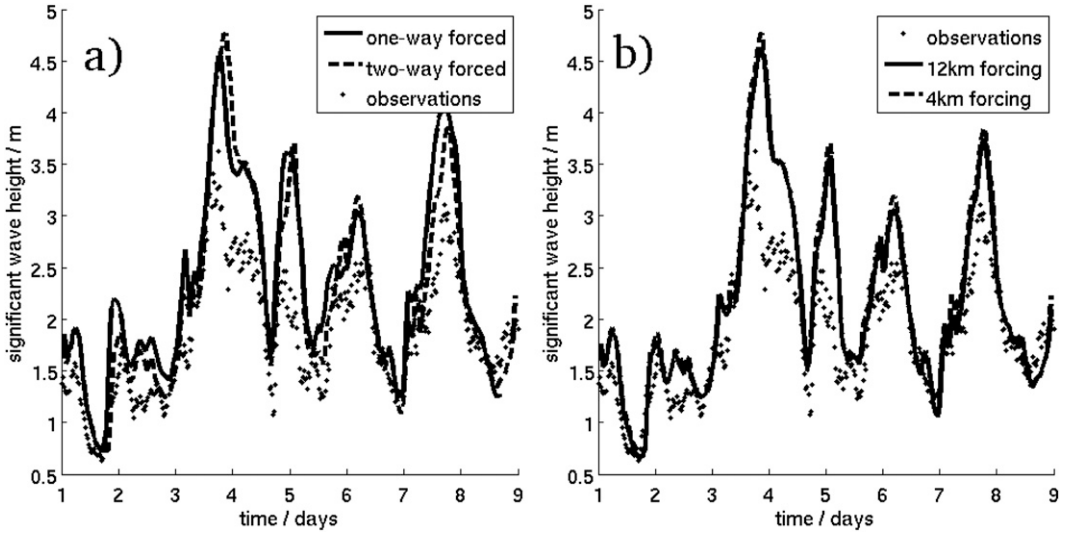

FIG. 7. Significant wave height at the Liverpool Bay buoy in the 1.8-km IRS ocean model comparing (a) one-way vs two-way coupling of meteorological model and (b) 12- and 4-km winds.

when they should be northwesterly). This is particularly seen at Hilbre Island, though it is lessened at a higher resolution. This further supports the use of the higher-resolution meteorological forcing for wave modeling.

A map of differences in wave heights in response to different resolutions of meteorological forcing is plotted in Fig. 9. The significant wave height is seen to increase (on average 7 cm) over the majority of the Irish Sea when the 4-km fields are used in place of the lower-resolution 12-km forcing. The modeled wave direction was also found to be sensitive to atmospheric model resolution. The impact on wave direction is more complicated than the direct effect of wind direction. In open water little difference is seen (Fig. 9; northward pointing vectors imply zero difference). Large directional differences (up to 38°) are seen in the eastern Irish Sea, in areas sheltered from the prevailing southwesterly winds. Wave directions are rotated in an anticlockwise direction by an average 5° when moving from 12- to 4-km resolution.

b. Surges

The ocean model was next used to calculate storm surge elevation at four sites. The modeled surge is sensitive to atmosphere–wave interaction; this effect has previously been discussed by Brown and Wolf (2009). Various methods of representing wave-generated surface roughness can be used in POLCOMS–WAM. Waves are effectively implicitly parameterized by using the formulation of Smith and Banke (1975), in which the drag coefficient increases with wind speed (though this was found to underestimate the wind stress). The Charnock formulation with a constant Charnock parameter is now commonly used in operational surge modeling (e.g., Williams and Flather 2000) giving a larger stress but requiring the Charnock parameter to be tuned to give optimum surge results. The coupled modeling system has the capability to include the waves explicitly in the surge model, using a dynamic two-way coupling. In this study, both methods were tested. In the 12-km ocean model, a constant Charnock parameter was implemented with a value of 0.0275, while in the 1.8-km-resolution model both a constant Charnock parameter of 0.0185 and a wave-related roughness were used. The modeled surge elevation was found to be sensitive to the way in which waves are represented by the model. This in turn suggests that the optimum drag coefficient may also vary with resolution, agreeing with the earlier findings of Brown and Wolf (2009).

Figure 10 shows modeled and observed surge elevations for four sites around Liverpool Bay. For the model runs shown, a Charnock parameterization was used in both cases. This result shows the sensitivity of the modeled surge to the ocean model component of the coupled system, as the meteorological forcing used was the same in these cases. Both the 12- and 1.8-km ocean models capture the variability of the observed surge, with the 12-km model overpredicting the surge elevation at all sites. The 1.8-km model is less consistent, overpredicting some surges and missing others. One obvious shortcoming was the overprediction of a large positive surge at all gauge sites at 0600 UTC 5 December 2006.

When run with a constant Charnock parameter, the 1.8-km model has a poorer R^2 correlation than that of

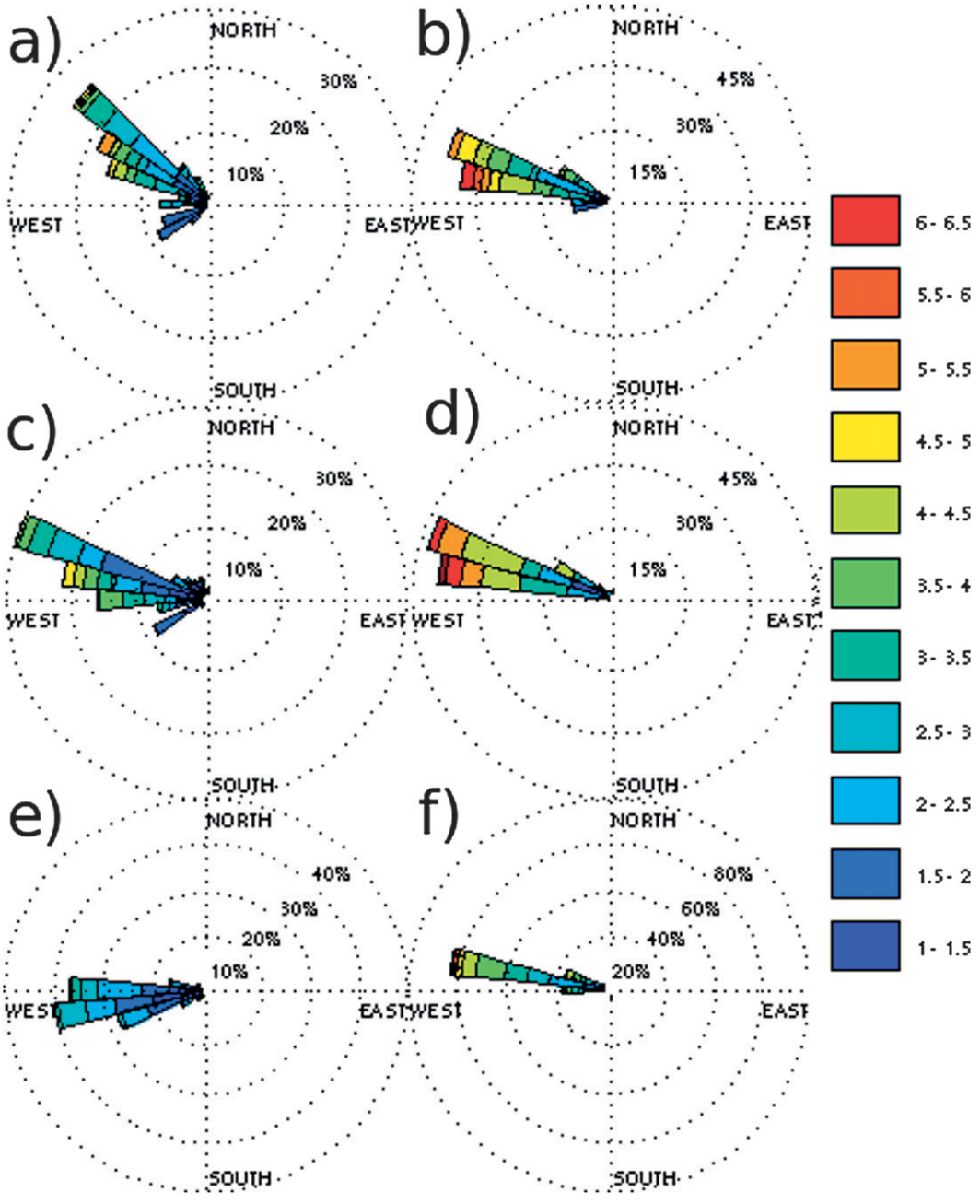

FIG. 8. Wave roses from (a),(c),(e) Liverpool Bay and (b),(d),(f) the Bristol Channel from the 12-km ocean model in (a) and (b) and the 1.8-km ocean model in (c) and (d). Compare with observations from wave buoys in (e) and (f).

the 12-km model (Table 7). Next, the wave model two-way coupling was tested in the 1.8-km ocean model. Adding the explicit representation of surface waves deteriorates the surge prediction in this case. Finally, surge model sensitivity to variable-resolution meteorological forcing was tested. The results from these experiments are not plotted, as little effect was seen: 12-km- and 4-km-resolution forcing were compared, giving virtually identical modeled surges. When the one-way nested meteorological model was applied at 12 and 4 km all surges remained within less than 0.5% of each other, and the two-way nested simulations were within 0.4% of each other. This may be because the local water level is governed equally by the incoming surge from the boundary and local atmospheric pressure, while the wave field is controlled by local winds.

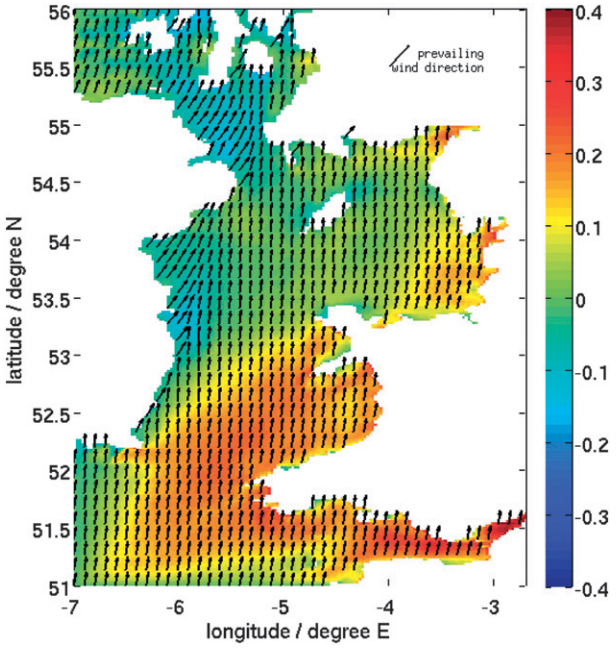

FIG. 9. Map of the mean difference in mean wave height (colors) and direction (vectors) in the Irish Sea when forced by winds from the 4-km minus winds from the 12-km WRF model. The mean difference across the full 9-day period is shown. The east–west component has been multiplied by 5 to clarify the change of direction.

c. *Communication and coupling*

By combining results from the wind, wave, and current models (normalized by their own means) in Fig. 11, we see how closely they are related. The calculation of a correlation between the modeled wind and wave time series gives $R^2 = 0.68$; between wave and surge the relationship is $R^2 = 0.66$ and $R^2 = 0.50$ for wind and surge.

The timings of peak events are also closely related, though some time lag can be seen. The peaks in wave height occur on average 5 h behind those of the wind field, while the surge model peaks on average 10 h later than the maximum winds. The variability of the wind field is less than that seen in the wave field, which is in turn less variable than the surge elevation.

So far the components of atmosphere and ocean have been considered separately but this is a little artificial as the meteorology is driving the ocean processes, and there are feedbacks. Running both model components locally gives the opportunity to specify the frequency of communication. In this study a fast (hourly) transfer of information from atmosphere to ocean was chosen. In operational modeling (e.g., Williams and Horsburgh 2010; You et al. 2010), 3-hourly winds are commonly used, which may not see such close correlation between the atmosphere and ocean as found here. Sensitivity to the frequency of meteorological forcing was tested in this configuration at 1-, 3-, 6-, and 12-hourly rates (not shown). Lower wave heights were found when applying lower-frequency wind forcing. Changing the forcing frequency from 1- to 3-hourly rates decreased the modeled wave height: the mean was reduced by around 4 cm and the maximum by 13 cm. When the frequency was further reduced (to 12 hourly), the significant wave height was decreased by a maximum of 2 m in the interior of the southern Irish Sea.

6. Discussion

The largest differences between modeled atmospheric wind speeds and directions, attributed to model resolution, are seen in the coastal zone. A likely reason for this difference is the representation of the coastline, as shown in Figs. 5d, 5e, and 5f. When the resolution of the atmospheric model is increased, the underlying terrain map also becomes more detailed. In the 12-km model the terrain is too smooth and slowly varying, with high peaks and sharp vertical gradients smoothed out. On increasing the resolution to 4 km (Fig. 5d), the coastline becomes sharper and more recognizable, resolving Anglesey and the Dee and Mersey estuaries. The north Wales mountains are also closer to their true heights, though the largest peaks are still missing. Further refinement in the highest-resolution domain (Fig. 5f) improves the picture further, with sharp topographic gradients generating larger pressure differences and faster winds (Fig. 5c).

Using higher-resolution meteorological forcing to drive the ocean model produced little impact on modeled surge elevation and wave height in Liverpool Bay. However, some structure appears in both surge and wave responses when the differences are mapped (Fig. 9). The largest differences in wave height (order 20 cm) are seen in the southern Irish Sea and in confined estuaries (in both areas, higher-resolution meteorological forcing leads to larger wave heights). The most extreme water levels in Liverpool Bay result from a combination of strong southwesterly winds, high waves, and a spring high tide. Under these circumstances, overtopping of coastal defenses and flooding are most likely to occur (Brown et al. 2010b). Wolf et al. (2011) found the 1.8-km Irish Sea model underestimated the wave height in Liverpool Bay, attributing this effect to an underestimate in model wind speed used as a forcing. Directional differences of up to 38° are seen in the eastern Irish Sea in areas sheltered from the prevailing southwesterly winds. Here, wave directions were found to be rotated in an anticlockwise direction when forced by the higher-resolution

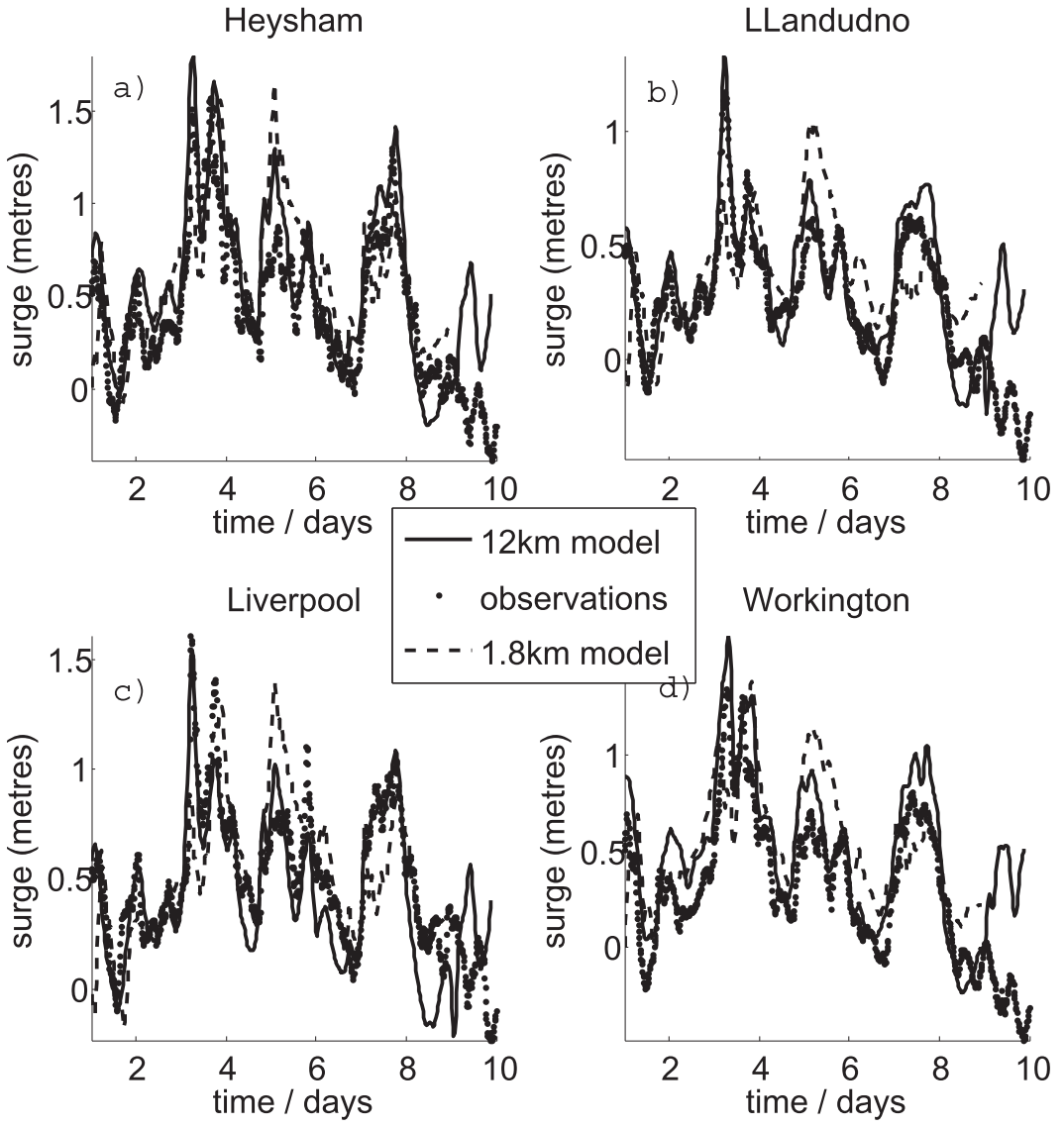

FIG. 10. Time series of surge elevation from four sites around the Irish Sea during December 2006. The 12-km surge-only model, 1.8-km surge-only model, and observations are compared.

winds. In these sheltered areas there will be little swell, and waves will be young. It naturally follows that the resolution of local wind forcing has the greatest impact where waves are locally generated.

The response of waves and surge to winds is examined in Fig. 11. The peak wave height lags peak wind speed by approximately 5 h, with the peak surge elevation another 5 h behind. Brown and Wolf (2009) found that

TABLE 7. The R^2, Pbias, and cost functions for tide plus surge elevation at four study sites at two different ocean model resolutions. In the models labeled "Charnock," wave effects on the surface roughness are parameterized through a Charnock (1955) relation or with a wave age related Charnock parameter (Janssen 2004).

	12-km Charnock			1.8-km Charnock			1.8-km coupled		
Location	R^2	Pbias	CF	R^2	Pbias	CF	R^2	Pbias	CF
Liverpool	0.69	12.34	0.36	0.52	0.30	1.45	0.23	35.91	0.56
Heysham	0.73	−33.35	0.43	0.47	−26.11	0.50	0.13	15.39	0.55
Llandudno	0.63	−26.95	0.37	0.31	−23.78	0.47	0.14	22.01	0.71
Isle of Man	0.67	14.48	0.33	0.30	20.49	0.46	0.20	−8.39	0.73

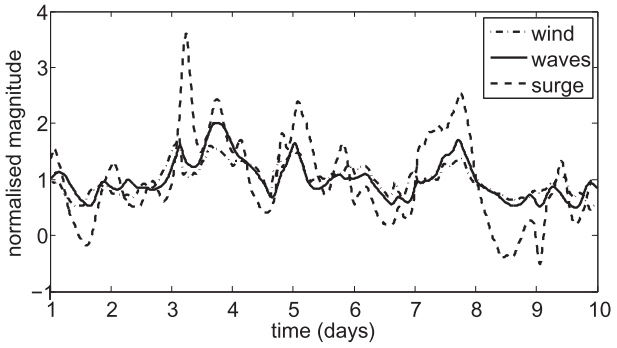

FIG. 11. Time series of wind speed at Hilbre Island (solid line), significant wave height at the Liverpool Bay buoy (dashed line), and storm surge elevation at Liverpool (dotted line) normalized by their own means.

during the 1977 surge event, wind stress peaks do not coincide with the times of peak surge and that the large tidal range in the eastern Irish Sea prevents the peak in surge occurring at the same time as the peak in wind stress. Instead, the maximum surge occurs on the rising tide. In the eastern Irish Sea, where a high tidal range and complicated coastal meteorology are combined, it is important to accurately represent the fast changing winds and tides with high temporal resolution. The differing response of wind, wave, and surge is also of interest. In Fig. 11a, a 1% change in wind speed translates into a 7% change in wave height and an 85% change in surge elevation. The energy in the system cascades down from the winds, through the waves and into the surge, and this illustrates the importance of the atmospheric field on driving the response of the ocean.

7. Future work

It would be interesting to extend this research into a period where waves are fetch limited. In fetch-limited conditions smaller wind waves are more dominant and the ocean conditions may be more sensitive to local winds. The test case used for this study covered a very stormy period, during which large waves built up over several hours. The presence of these larger waves may obscure any very small younger waves generated by local winds. These large waves approached from the west, without interruption from land. Future work could focus on winds blowing offshore and study how waves grow under these conditions.

Future model-development work should focus on developing a two-way coupling with feedbacks from ocean to atmosphere, as the authors believe this would strengthen coastal predictions (Warner et al. 2010). One drawback of our current work is the fact that variables are passed from the atmosphere to the ocean model but not in the other direction. There is also much work to be done at the atmosphere–ocean interface, improving the assumptions made to derive the ''10-m wind''; but by having control over all aspects of the coupled system, a better representation of this boundary layer will be possible. Bertotti et al. (2012) believe the most common problem in wave modeling is an overestimate of the wind speed and underestimated wave heights and suggest a stronger coupling is needed between atmosphere and ocean models.

8. Conclusions

The coupled WRF–POLCOMS–WAM modeling system is shown to be capable of representing the Liverpool Bay area, capturing high winds (around 25 m s^{-1}), large waves (up to 8 m), and surges (up to 1.5 m) during a simulated storm period. By increasing atmospheric model resolution, simulated wind speeds were seen to improve. The most notable improvement was observed when moving from 12- to 4-km resolution with errors in wind speed decreasing more than 10% on average. When moving from 4 to 1.33 km, little significant further improvement was observed in model wind speed correlations, and the use of two-way nesting showed no additional benefit.

Skill is also gained through forcing the ocean model with higher-resolution wind and pressure fields. The use of higher-resolution forcing was found to generally increase the wave height over the Irish Sea by up to 40 cm in places. Improved wave directions were also seen when 4-km meteorological forcing was used, with a focusing of waves into a more realistic narrower directional band. There was little response seen in the modeled surge when forced with increased resolution meteorological forcing.

This coupled modeling system is a useful test bed for the sensitivity of a model ocean to meteorological forcings. By forcing the ocean model with hourly meteorology, response times in the coupled system can also be observed. The ocean was found to respond sensitively to atmospheric forcing, with signals in wind speed being amplified in the ocean by between 7% and 85%. With the ability to control all modules of this system, an investigation was made into the importance of model resolution and coastal representation on nearshore winds, waves, and surges. This system now has potential to generate future work on the air–sea interface and feedbacks from ocean to atmosphere.

Acknowledgments. This work came about as a result of a visit to the Barcelona Supercomputing Centre, funded by the HPC–Europa Transnational Access Programme.

The overall project is part of FIELD_AC (FP7-SPACE-2009-1 242284). We acknowledge the United Kingdom Meteorological Office for providing data from the MIDAS land-based weather stations, RWE renewables npower for the Gwynt-y-mor data, and CEFAS for the use of their SmartBuoy data. The authors are also grateful to the contribution of anonymous reviewers who significantly improved the quality of the paper.

REFERENCES

Ardhuin, F., L. Bertotti, R.-R. Bidlot, L. Cavaleri, V. Filipetto, J.-M. Lefevre, and P. Wittmann, 2007: Comparison of wind and wave measurements and models in the western Mediterranean Sea. *Ocean Eng.,* **34,** 526–541.

Bertotti, L., and Coauthors, 2012: Performance of different forecast systems in an exceptional storm in the western Mediterranean Sea. *Quart. J. Roy. Meteor. Soc.,* **138,** 34–55.

Brown, J. M., and J. Wolf, 2009: Coupled wave and surge modelling for the eastern Irish Sea and implications for model wind-stress. *Cont. Shelf Res.,* **29,** 1329–1342.

——, A. Souza, and J. Wolf, 2010a: An 11-year validation of wave-surge modelling in the Irish Sea, using a nested POLCOMS-WAM modelling system. *Ocean Modell.,* **33,** 118–128.

——, A. J. Souza, and J. Wolf, 2010b: An investigation of recent decadal-scale storm events in the eastern Irish Sea. *J. Geophys. Res.,* **115,** C05018, doi:10.1029/2009JC005662.

Browning, K. A., 2004: The sting at the end of the tail: Damaging winds associated with extratropical cyclones. *Quart. J. Roy. Meteor. Soc.,* **130,** 375–399.

Bukovsky, M. S., and D. J. Karoly, 2009: Precipitation simulations using WRF as a nested regional climate model. *J. Appl. Meteor. Climatol.,* **48,** 2152–2159.

Caldwell, P., H.-N. Chin, D. C. Bader, and G. Bala, 2009: Evaluation of a WRF dynamical downscaling simulation over California. *Climatic Change,* **95,** 499–521.

Cavaleri, L., 2009: Wave modeling—Missing the peaks. *J. Phys. Oceanogr.,* **39,** 2757–2778.

Charnock, H., 1955: Wind stress on a water surface. *Quart. J. Roy. Meteor. Soc.,* **350,** 639–640.

Dudhia, J., 1989: Numerical study of convection observed during the winter monsoon experiment using a mesoscale two-dimensional model. *J. Atmos. Sci.,* **46,** 3077–3107.

Ek, M. B., K. E. Mitchell, Y. Lin, E. Rogers, P. Grunmann, V. Koren, G. Gayno, and J. D. Tarpley, 2003: Implementation of Noah land surface model advances in the National Centers for Environmental Prediction operational mesoscale Eta model. *J. Geophys. Res.,* **108,** 8851, doi:10.1029/2002JD003296.

Floors, R., E. Batchvarova, S. Gryning, A. N. Hahmann, A. Pena, and T. Mikkelsen, 2011: Atmospheric boundary layer wind profile at a flat coastal site—Wind speed lidar measurements and mesoscale modeling results. *Adv. Sci. Res.,* **6,** 155–159.

Gill, A., 1982: *Atmosphere–Ocean Dynamics.* Academic Press, 662 pp.

Heaps, N. S., 1983: Storm surges, 1967–1982. *Geophys. J. Roy. Astron. Soc.,* **74,** 331–376.

Hodur, R. M., 1997: The Naval Research Laboratory's coupled ocean/atmosphere mesoscale prediction system (COAMPS). *Mon. Wea. Rev.,* **125,** 1414–1430.

Holt, J. T., and D. J. James, 2001: An *s* coordinate density evolving model of the northwest European continental shelf: 1. Model description and density structure. *J. Geophys. Res.,* **106** (C7), 14 015–14 034.

Hong, S. Y., J. Dudhia, and S. Chen, 2004: A revised approach to ice microphysical processes for the bulk parameterization of clouds and precipitation. *Mon. Wea. Rev.,* **132,** 103–120.

——, Y. Noh, and J. Dudhia, 2006: A new vertical diffusion package with explicit treatment of entrainment processes. *Mon. Wea. Rev.,* **134,** 2318–2341.

Janssen, P. A. E. M., 2004: *The Interaction of Ocean Waves and Wind.* Cambridge University Press, 308 pp.

Jorba, O., T. Loridan, P. Jimenez-Guerrero, and J. M. Baldasano, 2008: Annual evaluation of WRF-ARW and WRF-NMM meteorological simulations over Europe. *Extended Abstracts, Ninth Annual WRF Users' Workshop,* Boulder, CO, NCAR, 8.3. [Available online at http://www.mmm.ucar.edu/wrf/users/workshops/WS2008/abstracts/8-03.pdf.]

Kain, J. S., 2004: The Kain–Fritsch convective parameterization: An update. *J. Appl. Meteor.,* **43,** 170–181.

Komen, G. J., L. Cavaleri, M. Donelan, K. Hasselmann, S. Hasselman, and P. Janssen, 1994: *Dynamics and Modelling of Ocean Waves.* Cambridge University Press, 556 pp.

Lennon, G. W., 1963: The identification of weather conditions associated with the generation of major storm surges along the west coast of the British Isles. *Quart. J. Roy. Meteor. Soc.,* **89,** 381–394.

Marrero, C., O. Jorba, E. Cuevas, and J. Baldasano, 2009: Sensitivity study of surface wind flow of a limited area model simulating the extratropical storm Delta affecting the Canary Islands. *Adv. Sci. Res.,* **2,** 151–157.

Maskell, J., 2012: Modelling storm surges in the Irish and Celtic seas using a finite element model (TELEMAC). Ph.D. dissertation, University of Liverpool, 280 pp.

Mass, C. F., D. Owens, K. Westrick, and B. A. Colle, 2002: Does increasing horizontal resolution produce more skillful forecasts? *Bull. Amer. Meteor. Soc.,* **83,** 406–430.

Met Office, cited 2013: North West England & Isle of Man: Climate. [Available online at http://www.metoffice.gov.uk/climate/uk/nw/print.html.]

Michalakes, J., J. Dudhia, D. Gill, T. Henderson, J. Klemp, W. Skamarock, and W. Wang, 2004: The Weather Research and Forecast model: Software architecture and performance. *Proc. 11th ECMWF Workshop on the Use of High Performance Computing in Meteorology,* Reading, United Kingdom, ECMWF, 1–13.

Miller, M., R. Buizza, J. Haseler, M. Hortal, P. Janssen, and A. Untch, 2010: Increased resolution in the ECMWF deterministic and ensemble prediction systems. *ECMWF Newsletter,* No. 124, ECMWF, Reading, United Kingdom, 10–16.

Mlawer, E. J., S. J. Taubman, P. D. Brown, M. J. Iacono, and S. A. Clough, 1997: Radiative transfer for inhomogeneous atmosphere: RRTM, a validated correlated-*k* model for the longwave. *J. Geophys. Res.,* **102** (D14), 16 663–16 682.

Monbaliu, J., R. Padilla-Hernandez, J. C. Hargreaves, J. C. Carretero Albiach, W. Luo, M. Sclavo, and H. Gunther, 2000: The spectral wave model, WAM, adapted for applications with high spatial resolution. *Coastal Eng.,* **41,** 41–62.

O'Neill, C. K., J. A. Polton, J. T. Holt, and E. J. O'Dea, 2012: Modelling temperature and salinity in Liverpool Bay and the Irish Sea: Sensitivity to model type and surface forcing. *Ocean Sci. Discuss.,* **8,** 903–913.

Osuna, P., and J. Wolf, 2005: A numerical study on the effect of wave-current interaction processes in the hydrodynamics of the Irish Sea. *Proc. Fifth Int. Conf. on Ocean Wave Measurement and Analysis: WAVES 2005,* Madrid, Spain, CEDEX, 10 pp.

Pickett, M., W. Tang, L. K. Rosenfeld, and C. H. Walsh, 2003: QuikSCAT satellite comparisons with nearshore buoy wind data off the U.S. West Coast. *J. Atmos. Oceanic Technol.,* **20,** 1869–1879.

Seo, H., A. J. Miller, and J. O. Roads, 2007: The Scripps coupled ocean–atmosphere regional (SCOAR) model, with applications in the eastern Pacific sector. *J. Climate,* **20,** 381–402.

Skamarock, W. C., and Coauthors, 2008: A description of the Advanced Research WRF version 3. NCAR Tech. Note NCAR/TN-475+STR, 113 pp.

Smith, S. D., and E. G. Banke, 1975: Variation of the surface drag coefficient with wind speed. *Quart. J. Roy. Meteor. Soc.,* **101,** 665–673.

Warner, J., C. Sherwood, R. Signell, C. Harris, and H. Arango, 2008: Development of a three-dimensional, regional, coupled wave, current, and sediment-transport model. *Comput. Geosci.,* **34,** 1284–1306.

——, B. Armstrong, R. He, and J. Zambon, 2010: Development of a Coupled Ocean-Atmosphere-Wave-Sediment Transport (COAWST) modeling system. *Ocean Modell.,* **35,** 230–244.

Williams, J. A., and R. A. Flather, 2000: Interfacing the operational storm surge model to a new mesoscale atmospheric model. POL Internal Document 127, 18 pp.

——, and K. J. Horsburgh, 2010: Operational storm surge forecasting with 3.5 km NISE10 model. POL Internal Document 199, 19 pp.

Wolf, J., 2008: Coupled wave and surge modeling and implications for coastal flooding. *Adv. Geosci.,* **17,** 1–4.

——, 2009: Coastal flooding: Impacts of coupled wave–surge–tide models. *Nat. Hazards,* **49,** 241–260.

——, and R. A. Flather, 2005: Modelling waves and surges during the 1953 storm. *Philos. Trans. Roy. Soc. London,* **363A,** 1359–1375.

——, J. M. Brown, and M. J. Howarth, 2011: The wave climate of Liverpool Bay observations and modelling. *Ocean Dyn.,* **61,** 639–655.

Wortley, S., E. Crompton, R. Orrell, D. Smith, K. Horsburgh, and J. A. Williams, 2007: Storm tide forecasting service: Operational report to the environment agency for the period 1st June 2006 to 31st May 2007. Met Office Tech. Rep., 67 pp.

You, S. H., W. Lee, and K. S. Moon, 2010: Comparison of storm surge tide predictions between a 2-D operational forecast system, the regional tide/storm surge model (RTSM), and the 3-D regional ocean modeling system (ROMS). *Ocean Dyn.,* **60,** 443–459.